

The Characteristics of Strain Induced Transformation in Medium Carbon Steels

CHEN CHIEN, YUAN-TSUNG WANG and CHING-YUAN HUANG

*Iron and steel Research & Development Department
China Steel Corporation*

In this study, the strain effects on the phase transformation and hardness of medium carbon steels (S50C) was investigated by using computer-aided steel simulation and the dilatometer. It has been well known that the deformation on austenite around Ar3 temperature has profound influences on the microstructure and the phase transformation evolution of the medium carbon steel. Therefore, the effects of different strain levels and deformation at different temperatures were discussed in this study. The microstructure as well as the hardness of the S50C steels were observed by OM/SEM and measured by Rockwell hardness test, respectively. It was found that as the strain energy increases, the volume fraction of ferrite and pearlite which replaces martensite, especially in the ferrite phase, these increases will result in the hardness of S50C steel to decrease significantly. The degree of grain refinement also elevates since the nucleation sites increase. When the applied energy is high enough, the pearlite colonies are broken into fragments, and the hardness drops further.

Keywords: Medium carbon steel, Martensite transformation, Grain refinement, Hardness, Dilatometer

1. INTRODUCTION

Medium carbon steels, by definition, have a carbon content larger than 0.2%. The steels have been widely applied in springs, spatulas, cutting tools, clampers, pins, and other parts which need to be abrasion resistant. It is because of the high carbon content in medium carbon steels that makes them stronger and harder to process⁽¹⁾. The most common way to make the medium carbon steels soft and formable is the spheroidization process⁽²⁻⁴⁾. However, the spheroidization process is energy and time consuming. Therefore, the long-term problem of medium carbon steel has been the excessive hardness leading to processing difficulties. To solve this problem completely, the increasing of the fraction of soft phases to reduce the hardness of medium carbon steels, like ferrite and pearlite, is necessary⁽⁵⁻⁸⁾. In this study, the deformation temperature and strain effects on the phase transformation of medium carbon steels (S50C) were investigated by using simulation and the quenching and deformation dilatometer.

2. EXPERIMENTAL METHOD

The chemical composition of the S50C steel was listed in Table 1. In this experiment, the phase evolution and property variation while applying different deformation temperatures and strain levels were investigated. In this investigation, the computer-aided steel

Table 1 Chemical composition of the S50C steel (in wt%)

C	Si	Mn	P	S
0.47~0.53	0.15~0.35	0.60~0.90	<0.030	<0.035

simulation was conducted first. The simulation predicted the transformation temperatures and critical cooling rate. Based on the phase transformation and microstructure, the simulation result also showed the hardness prediction. Because the core concept of this research was combining computer-aided steel simulation and different process routes by dilatometer, the thermal process routes were conducted by the quenching and deformation dilatometer DIL 805A/D. The dilatometer specimens were with a dimension of 5 mm in diameter and 10 mm in length.

Figure 1 shows the thermal cycle for the simulated thermo-mechanical treatment in the dilatometer. First, the specimen was heated to 1000°C, which was well above the austenitization temperature, for 180 seconds to get a full austenite structure. Then, the specimen was slowly cooled to three individual temperatures, and different deformation strains were applied as shown in Fig.1. Finally, the specimen was quenched to room temperature with a cooling rate of 60°C/s to preserve the microstructure.

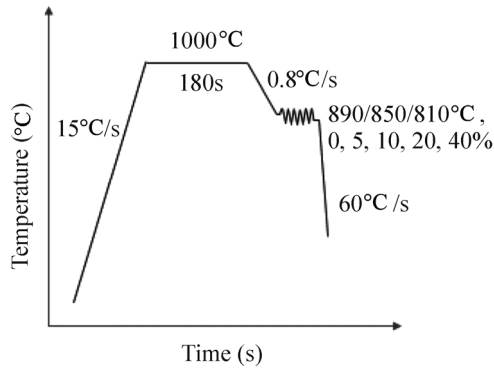


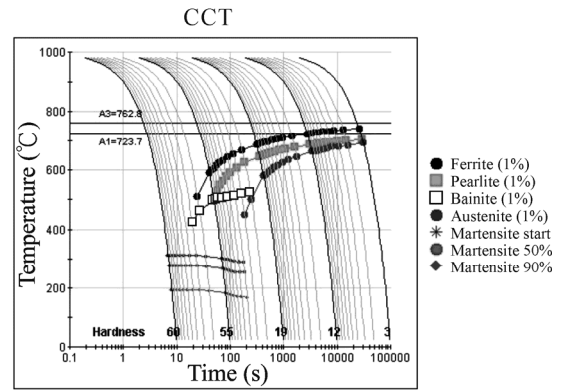
Fig.1. The thermal process route for the simulated thermo-mechanical treatment.

3. RESULTS AND DISCUSSION

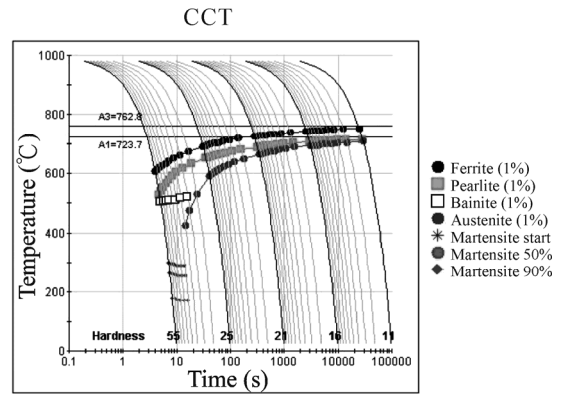
3.1 The computer-aided simulation results for different deformation strains

Figure 2 shows the computer-aided simulation results for different deformation strains. From Fig.2(a), with a cooling rate of $60^{\circ}\text{C}/\text{s}$ and no deformation strain applied, the ferrite and pearlite transformations will not occur. Therefore, the microstructure will be full martensite when the specimen is quenched to room temperature. However, when the low deformation strain is applied, for example 5% as shown in Fig.2(b), the Continuous Cooling Transformation (CCT) curves are shifted to the shorter time side. From Fig.2(b), we can predict the microstructure of the low deformation specimen is less martensite than with other phases, and the hardness is lower than that of the none deformation one because the ferrite and pearlite transformations happened when consuming the austenite. Actually, in the simulation result, the hardness of the none deformation specimen is 60 HRC and that of the low deformation specimen is 47 HRC.

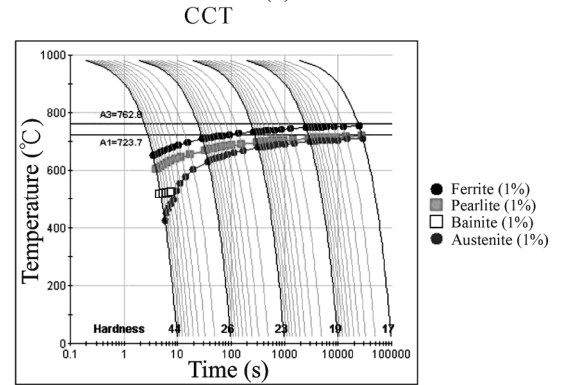
Figure 2(c) demonstrates the CCT curves when a high deformation strain is applied. As Fig.2(c) shows, the CCT curves are shifted to the much shorter time side, and the martensite transformation disappears. In this condition, none of the austenite leaves but transforms to martensite. From the simulation result in Fig.2(c), we can predict the microstructure of the high deformation specimen is lots of ferrite and pearlite phase present and almost no martensite shown, and the hardness must be lower than that of the none and low deformation ones. In the simulation of Fig.2(c), the hardness of the high deformation specimen is 33 HRC. In fact, the volume fraction of ferrite and pearlite phase of the high deformation specimen in Fig.2(c) is 13% and 87%, respectively.



(a)



(b)



(c)

Fig.2. The computer-aided steel simulation results of (a) no deformation strain, (b) low deformation strain, and (c) high deformation strain.

Figure 3 shows the calculation results of the Gibbs free energy and mass fraction of the with and without deformation specimens. When the specimen is under deformation, the Gibbs free energy will increase. By simulation software, we can apply strain energy to the austenite of the deformation specimen. Based on the thermodynamic theory, in the equilibrium state, the phase with the lowest Gibbs free energy will exist.

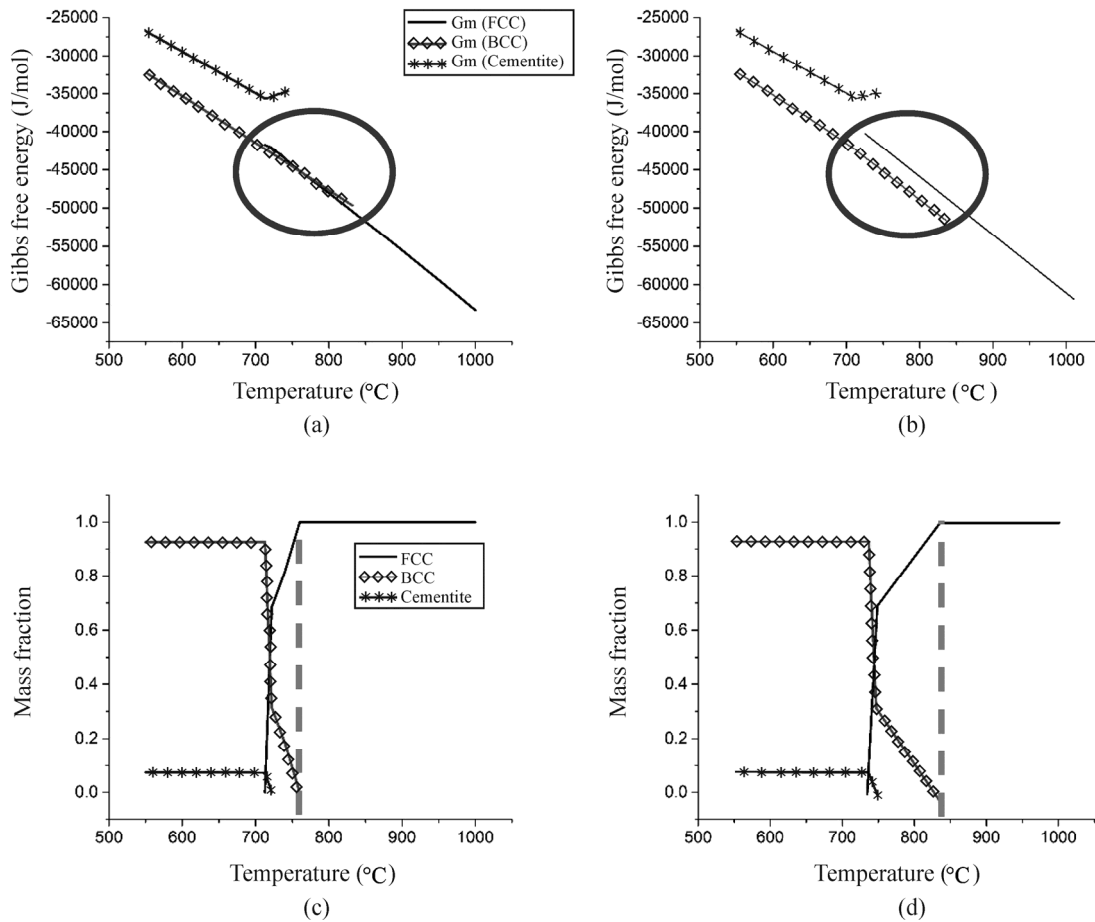


Fig.3. The calculation results of the Gibbs free energy and mass fraction of (a) and (c) without and (b) and (d) with deformation specimens, respectively.

From the circles in Fig.3(a)-(b), we can find the Gibbs free energy of FCC, which means the austenite, in the specimen with deformation has risen. The raised Gibbs free energy means that the stability of austenite is reduced. In other words, the austenite can not survive for the temperature below the dash line as shown in Fig.3(c)-(d). For the temperature below the dash line, the ferrite which has the lower Gibbs free energy will appear. Therefore, the ferrite will appear at a higher temperature as shown in Fig.3(d).

3.2 The metallographic images of different deformation strains and temperatures

Figures 4-6 are the metallographic images of different deformation strains at 890°C, 850°C and 810°C, respectively. In metallographic images, the white, bulk phase is martensite, and the dark phase is almost pearlite and ferrite. The metallograph of the deformation specimen shows other phases different from martensite, the dark phases. As the photos show that the volume fraction of martensite decreases as the deformation

strain increases is because the ferrite and pearlite transformations occur. In addition, one can observe from Figs.4-6 that the ferrite and pearlite appear as the deformation strain increases as shown in the zoom SEM images. The metallograph of high deformation specimen shows almost no martensite, especially in Fig.6. As compared with the simulation results from Fig.2, the hardness, measured by Rockwell hardness test, of the none deformation specimen, low deformation specimen and high deformation specimen are 57 HRC, 47 HRC and 30HRC, respectively. From metallographic images and the hardness, we can say the simulation results corresponds with the experimental data. Compared with Figs.4-6, it can be observed that at the lowest deformation temperature, the rate of decrease of martensite fraction and increase of ferrite/pearlite fractions are both the fastest, also shown in Fig.7. It can be observed that the more the effect of the deformation strain as the lower the temperature is. The reason of the phase evolution is the deformation strain can raise the Gibb free energy of austenite. Therefore,

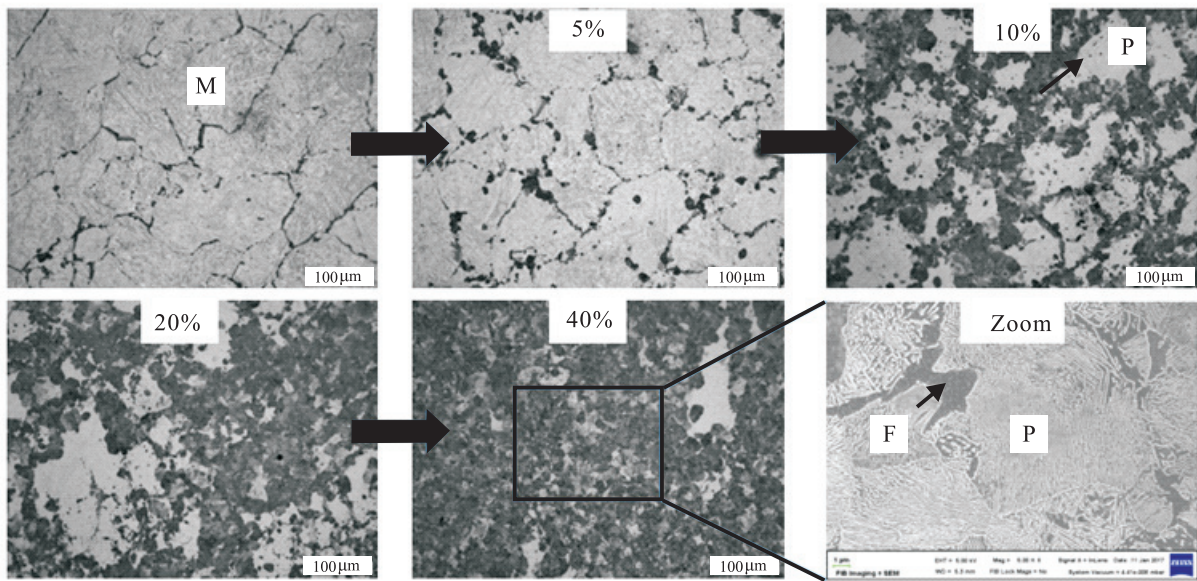


Fig.4. The metallographic images of different deformation strains at 890°C. In this images, phases were identified by M (martensite), P (pearlite) and F (ferrite), respectively.

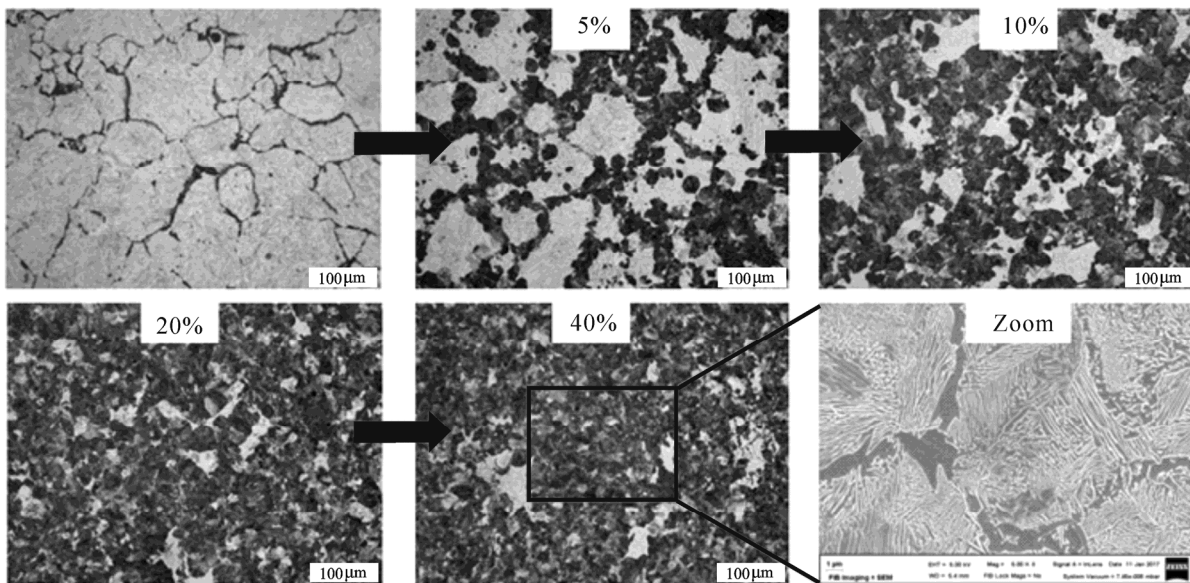


Fig.5. The metallographic images of different deformation strains at 850°C.

the austenite is so unstable that it can not survive for the martensite transformation. The effect of raising the Gibb free energy of austenite is more significant when the deformation temperature is lower because the austenite is the high temperature stable phase. It means the stability of austenite reduces as the temperature decreases. The deformation also reduces the Gibb free energy of ferrite and pearlite, especially the ferrite. That results in the increase of volume fraction of ferrite. In addition, the degree of grain refinement elevates

since the nucleation sites increase as the deformation strain energy increases. When the applied energy is high enough, the pearlite colonies are broken into fragments, and the hardness drops further as shown in the zoom SEM image in Fig.6. Figure 8 shows the summary of the experimental results. Where figure 8(a) shows that, the deformation strain can refine the grain size from 60 μm to 10 μm . The deformation strain also reduces the hardness, from 57 HRC to 30 HRC as shown in Fig.8(b).

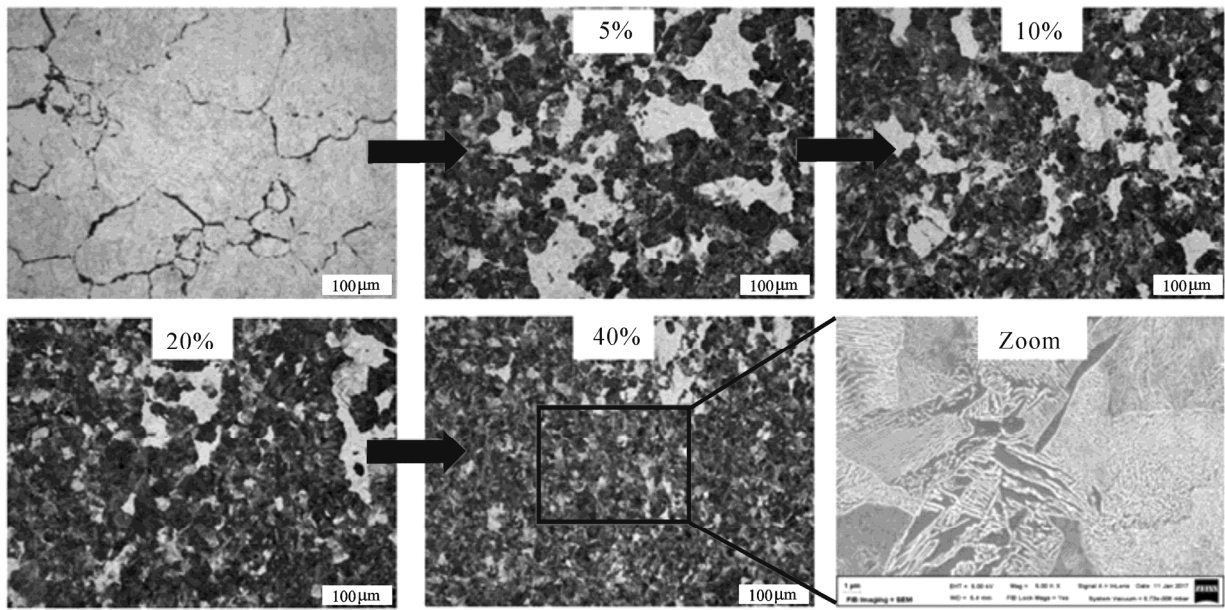


Fig.6. The metallographic images of different deformation strains at 810°C.

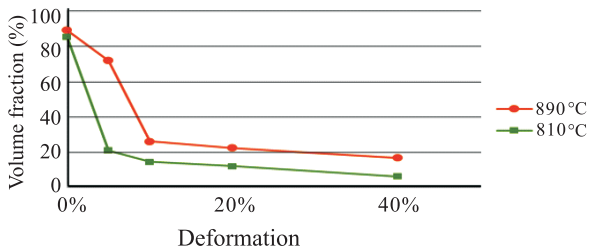


Fig.7. The volume fraction of white phase vs. deformation strain.

4. CONCLUSIONS

In this study, the deformation temperature and strain effects on the phase transformation of medium carbon steels (S50C) were investigated by using simulation and the quenching and deformation dilatometer. The microstructure as well as the hardness of the S50C steels were also provided. The deformation can shift CCT to a shorter time, refine the grain size and reduce the hardness significantly. In addition, the volume fraction of martensite decreases and that of pearlite and ferrite increases as the deformation strain increases. This is because the deformation strain can raise the

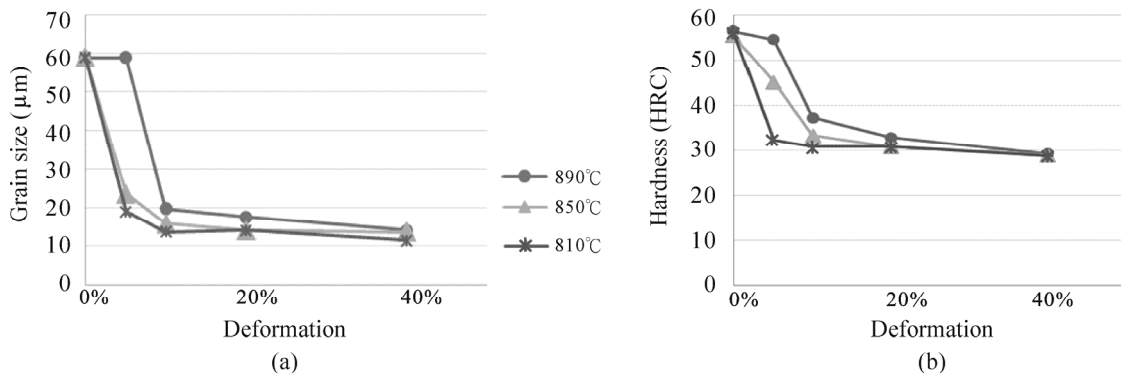


Fig.8. The summary of the experimental results: (a) grain size, (b) hardness vs. deformation strain.

Gibb free energy of austenite which is so unstable that it can not survive for the martensite transformation. The effect is more significant when the deformation temperature is lower. Fortunately, the simulation results highly corresponds with both the experimental data and metallographic images. This successful study of phase evolution provides us a clue to avoid martensite appearing. Therefore, the processing difficulties of medium carbon steel might be solved in the future.

REFERENCES

1. H. Yi, Z. Hou, Y. Xu, D. Wu and G. Wang: *Scripta Materialia*, 2012, vol. 67, pp. 645-648.
2. E. Karadeniz: *Materials & Design*, 2008, vol. 29, pp. 251-256.
3. A. Saha, D.K. Mondal and J. Maity: *Materials Science and Engineering: A*, 2010, vol. 527, pp. 4001-4007.
4. J. O'Brien and W.F. Hosford: *Journal of Materials Engineering and Performance*, 1997, vol. 6, pp. 69-72.
5. J. K. Choi, D. H. Seo, J. S. Lee, K. K. Um and W. Y. Choo: *ISIJ international*, 2003, vol. 43, pp. 746-754.
6. N. Park, S. Khamsuk, A. Shibata and N. Tsuji: *Scripta Materialia*, 2013, vol. 68, pp. 538-541.
7. S. Zhang, X. Sun and H. Dong: *Materials Science and Engineering: A*, 2006, vol. 432, pp. 324-332.
8. L. Hao, M. Sun, N. Xiao and D. Li: *Journal of Materials Science & Technology*, 2012, vol. 28, pp. 1095-1101. □